SCIENTIFIC REPORTS

OPEN

SUBJECT AREAS:
SENSORS
BIOANALYTICAL CHEMISTRY

Received
4 September 2014

Accepted
24 December 2014

Published
22 January 2015

Correspondence and requests for materials should be addressed to L.G. (guolh@fzu.edu.cn) or Z.L. (zylin@fzu.edu.cn)

Surface Enhanced Electrochemiluminescence of $Ru(bpy)_3^{2+}$

Daifang Wang, Longhua Guo, Rong Huang, Bin Qiu, Zhenyu Lin & Guonan Chen

Institute of Nanomedicine and Nanobiosensing; Ministry of Education Key Laboratory of Analysis and Detection Technology for Food Safety; College of Chemistry, Fuzhou University, Fuzhou, 350116, China.

Surface enhanced spectroscopy such as surface enhanced Raman spectrum (SERS) and surface enhanced fluorescence have been investigated extensively in the past two decades. Herein, we present experimental evidence to demonstrate the existence of a new surface enhanced spectroscopy, namely, surface enhanced electrochemiluminescence (SEECL). Our investigation indicates that the electrochemiluminescence (ECL) response of the $Ru(bpy)_3^{2+}$-tri-n-propylamine (TPrA) system could be significantly enhanced when the working electrode is modified with gold nanoparticle-SiO_2 core-shell nanocomposites (AuNP@SiO_2). It is worth noting that comparing with a working electrode modified with pure SiO_2 nanoparticles, the electrochemical responses of the two electrodes were quite similar, but the ECL signal of the AuNP@SiO_2 modified electrode was ~5 times higher than that of the SiO_2 nanoparticles modified electrode. Thus we infer that the localized surface plasmon resonance (LSPR) of the AuNPs could be a major contribution to the ECL enhancement. Our investigations also demonstrate that the ECL enhancement is closely related to the thickness of the SiO_2 layer. As much as 10 times ECL enhancement (comparing with the ECL intensity of bare electrode) is observed under the optimal conditions. The possible mechanism of the SEECL phenomenon is also discussed.

Confined and strongly enhanced electromagnetic fields can be excited when noble metal nanostructures are irradiated with electromagnetic waves[1]. The spectroscopy of molecules placed within these strongly enhanced electromagnetic fields can be dramatically enhanced, based on which, a novel branch of spectroscopy - surface enhanced spectroscopy is developed[2–4]. For example, SERS[5–7], surface-enhanced hyper-Raman spectroscopy[8–9], surface enhanced fluorescence[10–11], surface-enhanced second harmonic generation[12–14], and surface-enhanced infrared absorption spectroscopy[15–16] have been investigated extensively in the past two decades. Herein, we propose a novel surface-enhanced phenomenon to expend this fast-developing surface enhanced spectroscopy family. We present experimental evidences to demonstrate the existence of SEECL. The most widely used $Ru(bpy)_3^{2+}$ - TPrA ECL system is selected for a demonstration.

During the past several decades, ECL as a powerful analytical technique has attracted much attention in both the research and industrial communities[17–18]. Among all the ECL reagents, $Ru(bpy)_3^{2+}$ and its derivatives are the most representative and commonly used reagents due to their good water solubility, high electrochemical stability and the ability to be repeatedly regenerated in ECL reaction[19–20]. The $Ru(bpy)_3^{2+}$-ECL reaction system has been widely used in the areas of immunoassay[21–23], DNA quantification[24–26], pharmaceutical study[25,27] and environmental detection[28–29]. Except for the wide use of the $Ru(bpy)_3^{2+}$-ECL system in the scientific laboratories, the popularity of commercial ECL instruments, e.g. the Elecsys® platform developed by Roche Diagnostics, has favored the wide-spread applications of ECL technology in hospitals all over the world, which benefits millions of patients[30–31].

The ECL emission of $Ru(bpy)_3^{2+}$ alone is rather weak in solution. Therefore, in order to obtain high sensitivity, it is essential to find effective ways to enhance the ECL intensity of $Ru(bpy)_3^{2+}$. Hitherto, researchers have explored a variety of ways to enhance the ECL emission of $Ru(bpy)_3^{2+}$. These efforts include, 1) searching for the best coreactants based on their molecular structures[32]; 2) the investigation of different additives to enhance the ECL emission of $Ru(bpy)_3^{2+}$-TPrA system[33–34]; 3) the synthesis of novel ruthenium complexes, e.g., the synthesis of dual-core or multi-core ruthenium metal complexes[35–36]; and 4) the investigation of intramolecular electron transfer of the donor-acceptor systems[37–38]. However, up until now, the most successful ECL system is still the use of $Ru(bpy)_3^{2+}$, or its derivatives, as the emitting species and TPrA as the co-reactant. In fact, to date all commercially available ECL analytical instruments are based on $Ru(bpy)_3^{2+}$-TPrA ECL system. Thus the development of new approach to enhance the ECL emission of this ECL system could be potentially interesting for a variety of applications.

The first surface plasmon-coupled ECL is reported by Lakowicz and co-workers[39]. They found that the excited state of $Ru(bpy)_3^{2+}$ generated by electrochemical energy can excite the surface plasmon of a thin gold film coated on a glass substrate. In a subsequent work, they demonstrated that the surface plasmons of a thin continuous silver film can be excited by chemically induced excited luminophores[40]. These investigations indicated that, besides electromagnetic radiation, surface plasmon can also be excited by the excited state of luminophores. Recently, the interaction between the ECL of semiconductor nanocrystals and the LSPR of noble metal nanostructures has been investigated. Distance dependent quenching and enhancing of ECL is observed[41–42]. Although they didn't use the terminology of SEECL, these investigations could be the earliest findings of SEECL. However, no credible evidence is presented to distinguish the ECL enhancement derived from the recovery of the quenched ECL by forster energy transfer and those enhanced by the LSPR of metallic nanoparticles. In addition, hitherto, no detailed mechanism is proposed to explain this kind of ECL enhancement.

To the best of our knowledge, up until now, there are no literature on the use of the LSPR of noble metal nanostructures to enhance the emission of $Ru(bpy)_3^{2+}$-TPrA system. In this article, we demonstrate for the first time that the LSPR of AuNPs can effectively enhance the ECL emission of $Ru(bpy)_3^{2+}$-TPrA system. The following issues were investigated in details: 1) the exact evidence to demonstrate the existence of LSPR enhanced ECL of $Ru(bpy)_3^{2+}$; 2) the conditions to obtain best ECL enhancement; and 3) the possible mechanism of SEECL.

Results and discussion

The existence of SEECL. In order to show experimental evidence of SEECL, the ECL behaviors of five types of electrodes, namely, GE, GE/PDDA, GE/PDDA/AuNPs, GE/PDDA/AuNP@SiO_2 and GE/PDDA/SiO_2 were investigated. Herein, PDDA is utilized as a cationic polyelectrolyte to form a positively charged surface for the binding of the negatively charged AuNPs, SiO_2 nanoparticles and Au@SiO_2 nanoparticles. Figure 1 A shows the absorption spectra of AuNPs and AuNP@SiO_2. The LSPR peak of the as synthesized AuNPs was located at 528 nm. After wrapped by the silica shell, the absorption peak was red-shifted to 540 nm. It is worth to note that SiO_2 nanoparticles have no obvious absorption peak in this wavelength range (e.g. between 400 nm to 800 nm). Therefore, this 12-nm peak shift is generated by the SiO_2 modification, which changed the localized surface refractive index around the AuNPs. The refractive index of SiO_2 is 1.547, while it is 1.333 for H_2O. After SiO_2 modification, the refractive index around the AuNPs increased. Thus the LSPR peak was red-shifted[43–44]. The inset in Figure 1 A shows the typical TEM image of AuNP@SiO_2. The AuNP core was quasi-spherical and the diameter was ~25 nm, and the thickness of the silica shell is ~4 nm. It is worth to note that in order to present a comparable data, the size of AuNP@SiO_2 was close to the purchased SiO_2 nanoparticles. Figure 1 B depicts the electrochemical impedance spectroscopy (EIS) of various electrodes. It could be observed from the Nyquist plots that the electron transfer resistance (R_{ct}) at the surfaces of different electrodes increased after modification. The increase of R_{ct} is because that the electron transfer rate of PDDA and SiO_2 is worse than gold. In addition, the electronegative nanoparticles (e.g. AuNPs, SiO_2 nanoparticles and AuNP@SiO_2) would repel the electronegative $Fe(CN)_6^{3-/4-}$ hence a higher R_{ct} is observed. The different EIS responses indicate the successful modification of different nanoparticles onto the electrodes.

Figure 2 Ashows the ECL responses of different modified electrodes in a same ECL solution containing 5 μmol/L $Ru(bpy)_3^{2+}$ and 0.5 mmol/L TPrA. The results show that slight decrease of ECL emission is observed after the modification of the electrode with AuNPs. This kind of ECL decrease should be attributed to the energy transfer between gold nanoparticles and $Ru(bpy)_3^{2+}$. It is well-known that $Ru(bpy)_3^{2+}$-TPrA system reacts at the surface of the working

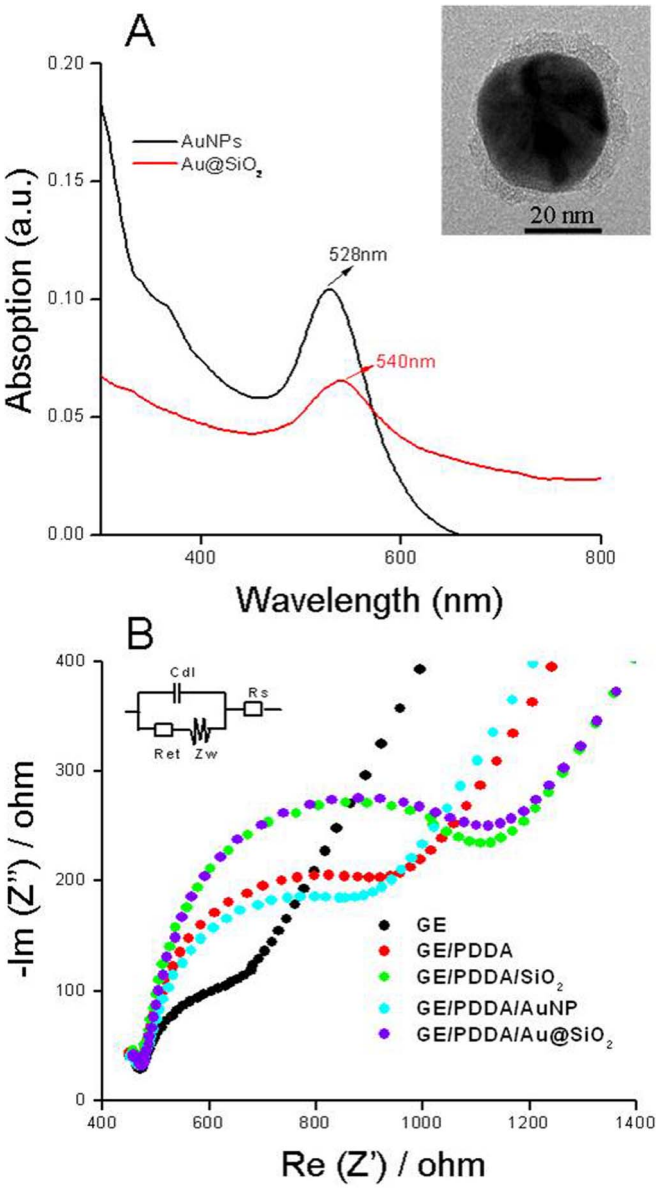

Figure 1 | (A) UV-vis adsorption spectra of AuNPs before and after silica coating. The inset shows the TEM image of a typical nanoparticle of AuNP@SiO_2; (B) Nyquist plots of different modified electrodes.

electrode to generate the excited-state $Ru(bpy)_3^{2+}$*. The light emission was observed when excited-state $Ru(bpy)_3^{2+}$* return to its ground state ($Ru(bpy)_3^{2+}$). However, in case of the presence of gold nanoparticles, it is possible to observe the energy transfer from $Ru(bpy)_3^{2+}$* to gold nanoparticles, and there is no light emission in this case. Therefore, ECL quenching was observed[45–46]. This kind of energy transfer can be effectively prevented after coating the AuNPs with SiO_2. As shown in Figure 2 A, the ECL intensity of electrode modified with AuNP@SiO_2 was significantly increased comparing to both the PDDA and AuNP modified electrodes. This kind of ECL enhancement could be attributed to the following two aspects. First, modification of nanoparticles to GE would increase the surface area of the electrode (the so called "nanoelectrode" effect), which means that more $Ru(bpy)_3^{2+}$ could react at the surface. In order to disclose how much ECL enhancement could be generated by this kind of "nanoelectrode" effect, we investigated the ECL behavior of SiO_2 nanoparticle modified GE. Since the size of SiO_2 nanoparticle was similar to AuNP@SiO_2 nanoparticles, and the electrochemical responses of the two modified electrodes were

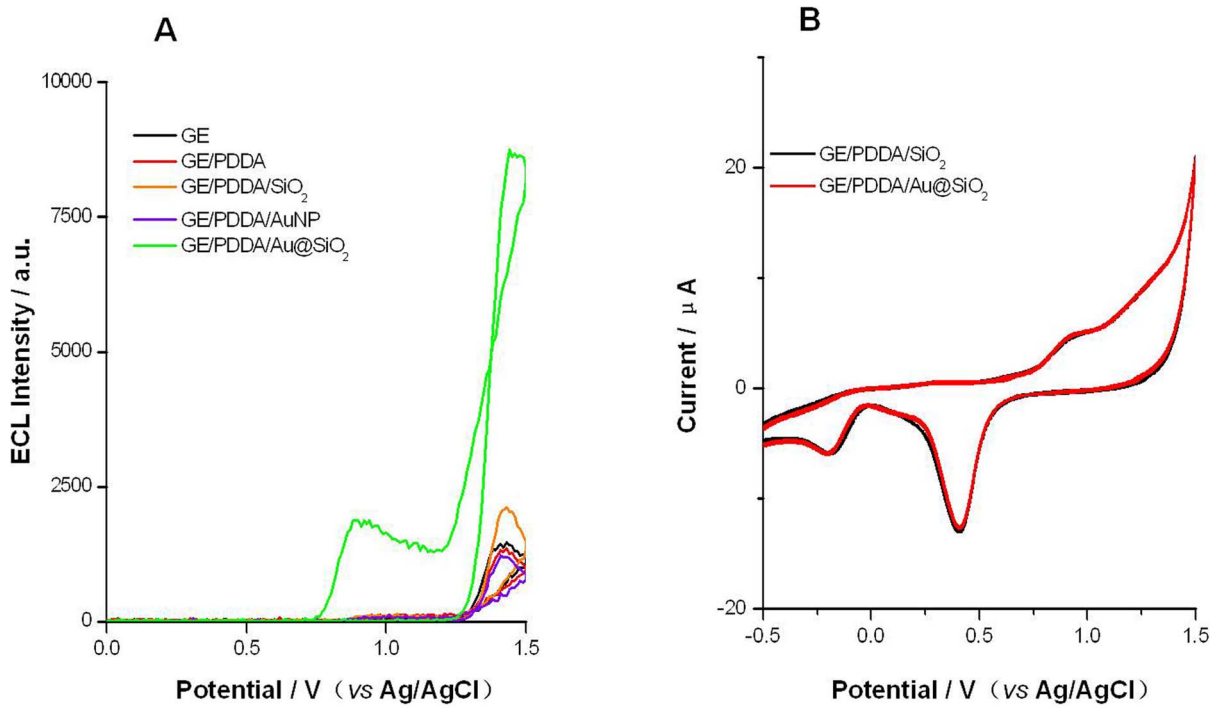

Figure 2 | (A) ECL emission of GE (blank),GE/ PDDA (red), GE/PDDA/SiO_2 (orange), GE/PDDA/AuNPs (violet) and GE/PDDA/AuNP@SiO_2 (green, the thickness of the silica shell is ~4 nm); (B) Simultaneous electrochemical current measurement of GE/PDDA/SiO_2 (black) and GE/PDDA/AuNP@SiO_2 (red).

almost the same (Figure 2 B), the nanoelectrode effect of the two electrodes should be similar, too. However, it can be clearly seen from Figure 2 A that the ECL intensity of the AuNP@SiO_2 modified GE was much higher than the one modified with SiO_2 nanoparticles. Therefore, except for the nanoelectrode effect, a second factor should be attributed to the ECL enhancement. Because of the only difference between the two electrodes are the modification materials: one is AuNP@SiO_2 and the other is SiO_2 nanoparticles. We conjectured that this kind of ECL enhancement should be own to the LSPR of AuNPs.

Conditions to obtain best ECL enhancement. We investigated the effect of the thickness of SiO_2 shell to the ECL enhancement. The silica shell thickness of AuNP@SiO_2 was controlled by adjusting the dosage of TEOS used in the synthetic reaction, and the typical TEM images representing the relationship between the dosage of TEOS

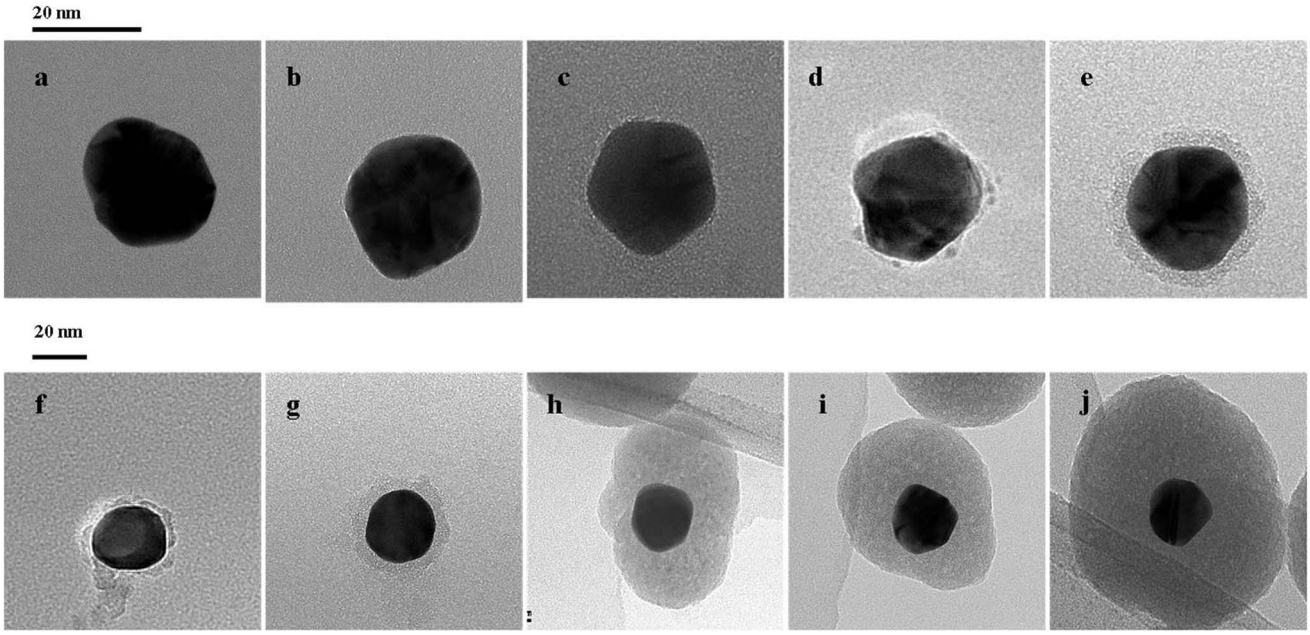

Figure 3 | **Typical TEM images of AuNP@SiO_2 nanoparticles with different shell thickness.** The volume of TEOS used in **a** to **k** are 2 μL, 4 μL, 6 μL, 8 μL, 10 μL, 12 μL, 14 μL, 16 μL, 18 μL, and 20 μL, respectively.

and silica shell thickness are shown in Figure 3. When the amount of TEOS varied from 0 μL to 20 μL, the shell thickness increased from 0 nm to ~30 nm. Next, we investigated the relationship between the shell thickness and the ECL enhancement. The results shows that the ECL intensity varied with the SiO_2 shell thickness of AuNP@SiO_2 (figure 4 A). When the SiO_2 shell thickness varied from 0 to 2 nm, only slight ECL enhancement was observed. When the SiO_2 shell thickness was more than 2 nm, the ECL intensity enhanced significantly with the SiO_2 shell thickness. Best ECL enhancement was observed with a SiO_2 shell thickness of 6 nm. It should be noted that instead of ECL enhancement, further increase the shell thickness induced ECL decrease. We infer that there are two major interactions between AuNPs and $Ru(bpy)_3^{2+}$: ECL quenching induced by energy transfer between the luminophors (e.g. $Ru(bpy)_3^{2+}$) and AuNPs, and LSPR-field enhancement of ECL. Therefore, the ECL emission is the competition result of these two effects. When AuNPs approach to $Ru(bpy)_3^{2+}$ closely, energy transfer will play the leading role and ECL could be quenched significantly. Energy transfer between the luminophors and AuNPs decrease rapidly with the increase of SiO_2 shell thickness. Thus LSPR-field enhancement of ECL is the dominant factor when the shell thickness increases from 2 nm to 6 nm, resulting in significant ECL enhancement. However, further increase the SiO_2 shell thickness induced rapid ECL intensity decrease. This is due to the reason that the LSPR electromagnetic field decaying exponentially with distance[47–48]. Therefore, the LSPR-field induced ECL enhancement weakened with the shell thickness increase from 6 nm to 30 nm. When the shell thickness increased to 30 nm, the ECL intensity of electrode modified with AuNP@SiO_2 was similar to the one modified with SiO_2 nanoparticle, suggesting that the LSPR-field induced ECL enhancement disappeared in that case (Figure S2). Based on the above discussion, a shell thickness of 6 nm was selected as the optimal condition to obtain maximum ECL enhancement.

Stability and reproducibility of SEECL. The stability and reproducibility of the AuNP@SiO_2 induced ECL enhancement is vital important for analytical application of this phenomenon. The stability of SEECL can be evaluated by repeatedly testing the ECL signal from a same AuNP@SiO_2 modified electrode, while the reproducibility of SEECL can be evaluated by testing the ECL signal of different AuNP@SiO_2 modified electrodes collected from different batches. As it can be seen from Figure S5, the RSD of ECL response is 4.2% (n = 8) for a same AuNP@SiO_2 modified electrode, and 6.2% for five AuNP@SiO_2 modified electrodes collected from 5 different batches. The good stability and reproducibility of SEECL indicate the great potential for utilizing the method for ECL signal enhancement. We believe that better uniformity and reproducibility of AuNP@SiO_2 modification were obtained by using a fully-immersed approach instead of the conventional drop-and-dry method for the preparation of AuNP@SiO_2 modified electrodes. The good uniformity and reproducibility greatly improved the stability and reproducibility of the ECL enhancement.

Mechanism of SEECL. Finally, we try to discuss the possible mechanism behind SEECL. Although previously there are few works described that the ECL of CdS thin films can be enhanced by gold nanoparticles[42,49], no credible evidence was presented to distinguish the ECL recovered from the quenched ECL by forster energy transfer and the ECL enhanced by the LSPR of metallic nanoparticles. In addition, up until now, no detailed mechanism is proposed to answer for this kind of ECL enhancement. Herein, we propose a three-step mechanism to summarize the phenomenon of SEECL as follows (Figure 5):

The first step is the generation of excited state of luminophors (e.g. $Ru(bpy)_3^{2+}$* in our case) via electrochemical reaction. The electrochemical generation of ground state $Ru(bpy)_3^{2+}$ to excited state $Ru(bpy)_3^{2+}$* via TPrA is presented in other literatures[50], and it is also depicted in Figure 5 (the green route).

The second step involves the generation of plasmon resonance at the surface of AuNPs. Lakowicz and co-workers[39] demonstrated that the excited state of $Ru(bpy)_3^{2+}$ generated by electrochemical energy can excite the surface plasmon of a thin gold film coated on a glass

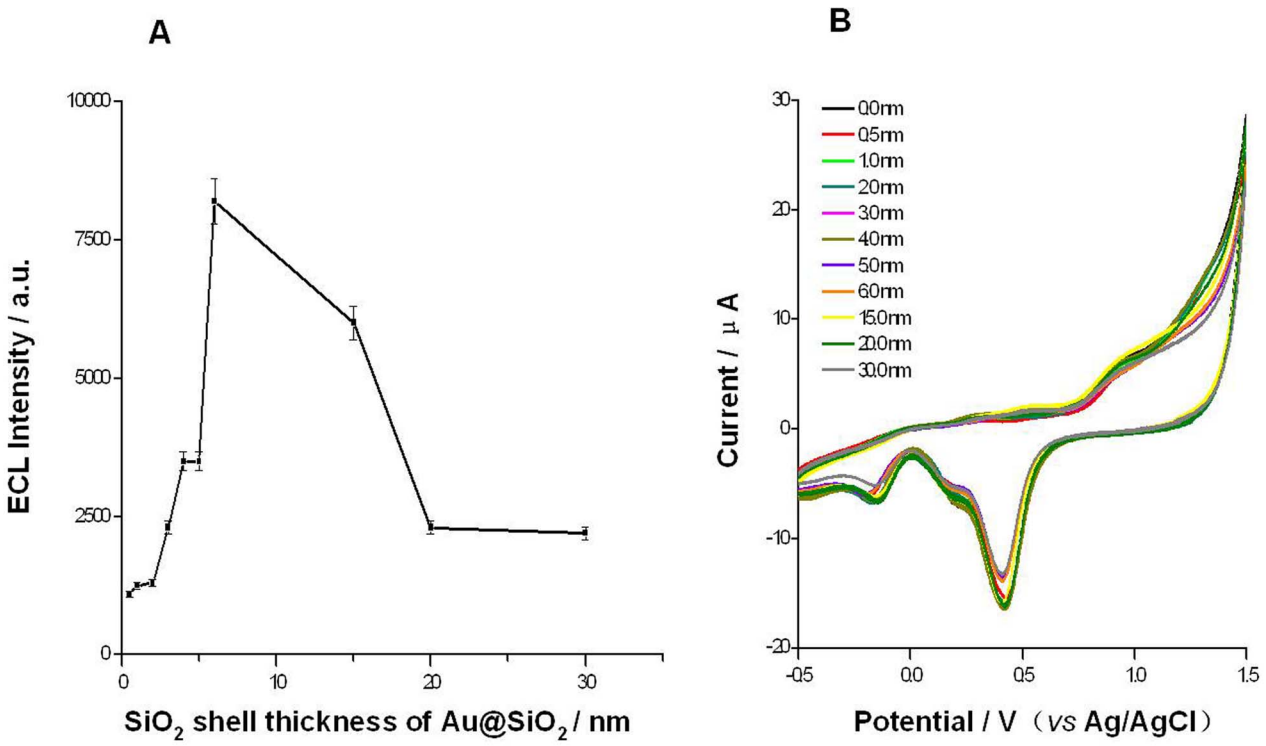

Figure 4 | (A): Relationship between ECL intensity of AuNP@SiO_2 modified electrodes and the silica shell thickness. Error bars represent standard deviations of 5 replicates; (B): The simultaneous measurement of the electrochemical current at AuNP@SiO_2 modified electrodes.

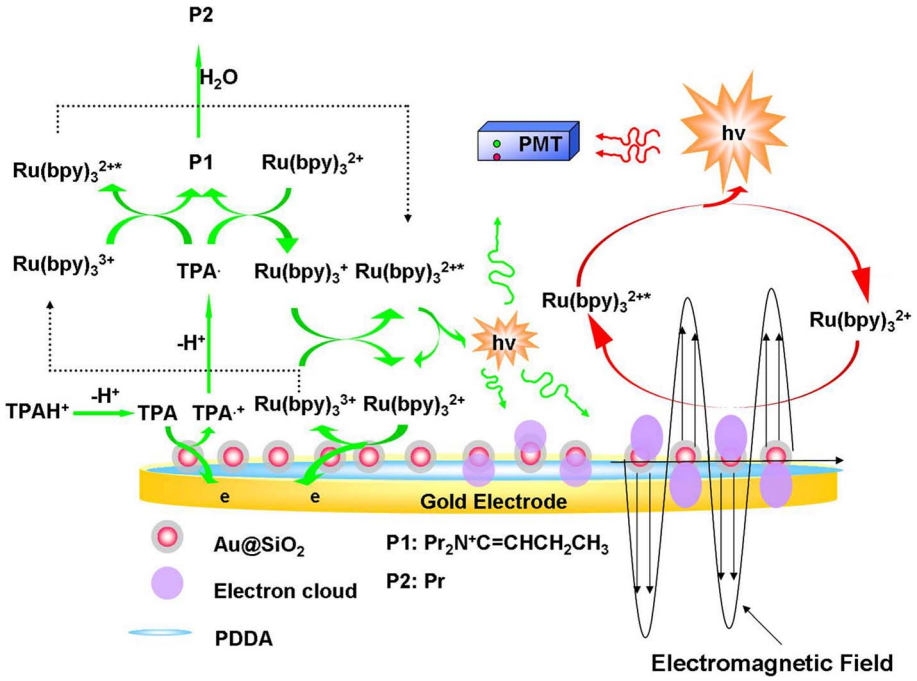

Figure 5 | **The schematic diagram of SEECL.**

substrate. This investigation suggests that besides electromagnetic radiation, surface plasmon can also be excited by the excited state of luminophores. Although their investigation was based on ECL generated propagating surface plasmon resonance, it is predictable that LSPR could also be generated after changing the thin noble metal film into AuNPs.

After the generation of SPR, the last question is how the SPR enhances the ECL emission. Similar to fluorescence, the ECL efficiency can be characterized by the gain in the relative molecular detection efficiency (MDE). MDE(r_0) at a position r_0 can be defined by the following equation[51]:

$$\mathrm{MDE}(r_0) = \underbrace{\Gamma_{\mathrm{exc}}(r_0)}_{\text{Excitation}} \times \underbrace{Q \times \mathrm{MCE}(r_0)}_{\text{Emission}} \qquad (1)$$

Where $\Gamma_{exc}(r_0)$ is the excitation rate, Q is the ECL quantum yield, and MCE(r_0) is the molecular collection efficiency function at point r_0.

It is well-known that LSPR would produce strong electromagnetic field near the surface of the metal nanoparticle. Thus we propose that this kind of strong electromagnetic field could increase both the excitation rate ($\Gamma_{exc}(r_0)$) and the emission factor ($Q \times$ MCE(r_0)) in eqn. 1. The reason that we propose this mechanism is based on the following facts:

First, it is reported that luminophores can be excited either by a propagating or an evanescent electromagnetic field[52–53]. Since LSPR induced electromagnetic field is belong to evanescent electromagnetic field, it is reasonable that this kind of electromagnetic field can excite the ground state luminophores (e.g. $Ru(bpy)_3^{2+}$) to the excited state (e.g. $Ru(bpy)_3^{2+}$*), as a result, the excitation rate ($\Gamma_{exc}(r_0)$) is increased.

Second, the electromagnetic field generated by the LSPR can also tune the emission factor ($Q \times$ MCE(r_0)) by reducing the fluorescence lifetime and in an increase of the quantum efficiency of the fluorophores, which is extensively investigated in surface enhanced fluorescence and it is well-known as the radiative decay engineering (RDE)[54]. Since the emission state of $Ru(bpy)_3^{2+}$ for fluorescence and ECL is the same ($Ru(bpy)_3^{2+}$*), and RDE is based on engineering the emission only, it is predictable that the electromagnetic field can also increase the emission factor ($Q \times$ MCE(r_0)) of $Ru(bpy)_3^{2+}$*.

In summary, LSPR induced ECL enhancement is accomplished by increasing both the excitation rate ($\Gamma_{exc}(r_0)$) and the emission factor ($Q \times$ MCE(r_0)) of luminophores. It is worth to note that the above mechanism is mainly deduced from previous theories. More experimental data, e.g. the relationship between SEECL and nanoparticle size, shape, interparticle distance, and LSPR spectrum, should be present in the near future to testify the validity of the proposed mechanism.

Conclusion. In summary, a novel surface enhanced spectroscopy - SEECL was reported in this work. Our investigation demonstrated that the modification of AuNP@SiO_2 onto the surface of the working electrode could generate significant ECL enhancement for the $Ru(bpy)_3^{2+}$-TPrA ECL system. This kind of ECL enhancement is attributed to the LSPR of AuNPs. We inferred that the strong electromagnetic field generated by the LSPR of AuNPs could increase both the excitation rate ($\Gamma_{exc}(r_0)$) and the emission factor ($Q \times$ MCE(r_0)) of $Ru(bpy)_3^{2+}$, as a consequence, the ECL emission is greatly enhanced. Our investigation also revealed that controlling inter-distance between $Ru(bpy)_3^{2+}$ and the surface of AuNPs is necessary to obtain best ECL enhancement. Although only the ECL system of $Ru(bpy)_3^{2+}$-TPrA is investigated herein, it is optimistic to predict the versatile of the approach because it is reasonable to expend SEECL to other inorganic, organic and semiconductor nanocrystal ECL systems.

Methods

Apparatus and Reagents. The ECL measurements were recorded by a model BPCL-1-TIC ultra weak luminescence analyzer. The electrochemical measurements were conducted by a CHI 660D electrochemical workstation. All experiments were carried out with a conventional three-electrode system. The reference electrode was a Ag/AgCl electrode, the working electrode was a gold electrode (φ = 2 mm) or a nanoparticle-modified gold electrode, and a piece of Pt wire was used as the counter electrode. The UV-vis absorption spectra were obtained on a Shimadzu UV-3600 UV-vis-NIR photospectrometer. Tris(2,2′-bipyridyl)dichlororuthenium (II) hexahydrate ($Ru(bpy)_3Cl_2{\cdot}6H_2O$) and SiO_2 nanoparticles (~30 nm diameter) were used without further purification. Hydrogen tetrachloroaurate tetrahydrate ($HAuCl_4{\cdot}4H_2O$), ethyl silicate (TEOS), Poly (diallydimethlammonium chloride) (PDDA), sodium dodecyl sulfate (SDS), TPrA and dibutylaminoethanol (DBAE) were of analytical grade and were used as received. Millipore ultrapure water (resistivity ≥18.2 MΩcm) was used throughout.

Synthesis of AuNP@SiO_2 nanoparticles. AuNPs were synthesized by an approach based on seed-mediated nanoparticle growth[55]. The average diameter of these synthesized AuNPs was ~25 nm. Silica coating of the AuNPs was adopted from a previous report[56]. Briefly, Aliquot 20% (v/v) TEOS-ethanol solution was injected to the mixture solution of 2 mL as-synthesized AuNP solution and 0.02 mL 0.1 M NaOH with vigorous stirring at 25°C. The dosage of TEOS for each injection is 2 μL. The injection volumes for sample number 1 to 9 were 2 μL, 4 μL, 6 μL, 8 μL, 10 μL, 12 μL, 14 μL, 16 μL, and 18 μL, respectively. The mixture solution was then incubated at 25°C for 24 hours. The solution was centrifuged at 7000 rpm for 10 min and the precipitate was redispersed in H_2O for further characterization.

Preparation of different nanoparticle-modified electrodes. Gold electrodes were polished to a mirror finish with 0.5 μm and 0.05 μm of alumina aqueous slurry in turn. The bare gold electrodes were then immersed in 50% (v/v) HNO_3 for 3 min under sonication; next, the electrodes were taken out and washed with doubly distilled water, then soaked in 50% (v/v) ethanol for 3 min under sonication; the electrodes were then immersed into doubly distilled water for another 3 min under sonication. The electrodes were electrochemically scanned with cyclic voltammetry (CV) in a potential range from −0.4 V to +1.6 V in 0.5 M H_2SO_4 solution for 10 times until steady CV curves were obtained. Then the electrodes were immersed into an aqueous solution containing 3 mg/ mL PDDA for 30 min. The electrodes were then washed with distilled water to obtain the PDDA modified electrodes. For the preparation of SiO_2 nanoparticles modified electrode, the PDDA modified electrode was placed into a solution containing negatively charged SiO_2 nanoparticles and was allowed to incubate for 30 min. The SiO_2 nanoparticle-modified electrode was then carefully washed with water to remove the unstably adsorbed SiO_2 nanoparticles to obtain the SiO_2 modified electrode (GE/PDDA/SiO_2). Similarly, AuNP modified electrode (GE/PDDA/AuNPs) and AuNP@SiO_2 modified electrode (GE/PDDA/AuNP@SiO_2) were obtained by immersing the PDDA modified electrodes into the AuNP solution and AuNP@SiO_2 solution, respectively.

ECL measurements. A 5.0 mL cylindroid glass cell was used as an ECL cell, which was successively washed with 0.5 M HNO_3 and doubly distilled water, and dried in an oven before use. All the modified electrodes were used as working electrodes and immersed into a 1.0 mL solution containing 0.1 M pH 9.5 phosphate buffer solution (PBS), 5 μmol/L $Ru(bpy)_3^{2+}$ and 0.5 mmol/L TPrA for ECL measurement. The CV and ECL spectroscopy were recorded between −0.5 V and +1.5 V at a scan rate of 100 mV/s. ECL signal was measured with an ultra weak luminescence analyzer at room temperature, and the voltage of the PMT was set at 1000 V. All measurements were performed at room temperature.

1. Saha, K., Agasti, S. S., Kim, C., Li, X. & Rotello, V. M. Gold nanoparticles in chemical and biological sensing. *Chem. Rev.* **112**, 2739–2779 (2012).
2. Moskovits, M. Surface-enhanced spectroscopy. *Rev. Mod. Phys.* **57**, 783 (1985).
3. Alonso-González, P. *et al*. Resolving the electromagnetic mechanism of surface-enhanced light scattering at single hot spots. *Nat. Commun.* **3**, 684 (2012).
4. Mayer, K. M. & Hafner, J. H. Localized surface plasmon resonance sensors. *Chem. Rev.* **111**, 3828–3857 (2011).
5. Nie, S. & Emory, S. R. Probing single molecules and single nanoparticles by surface-enhanced Raman scattering. *Science* **275**, 1102–1106 (1997).
6. Zhang, R. *et al*. Chemical mapping of a single molecule by plasmon-enhanced Raman scattering. *Nature* **498**, 82–86 (2013).
7. Lombardi, J. R. & Birke, R. L. A unified view of surface-enhanced Raman scattering. *Accounts of chemical research* **42**, 734–742 (2009).
8. Milojevich, C. B., Silverstein, D. W., Jensen, L. & Camden, J. P. Probing two-photon properties of molecules: Large non-Condon effects dominate the resonance hyper-Raman scattering of rhodamine 6g. *J. AM. CHEM. SOC.* **133**, 14590–14592 (2011).
9. Kneipp, J., Kneipp, H. & Kneipp, K. Two-photon vibrational spectroscopy for biosciences based on surface-enhanced hyper-Raman scattering. *P. Natl. Acad. Sci.* **103**, 17149–17153 (2006).
10. Guerrero, A. R. & Aroca, R. F. Surface-Enhanced Fluorescence with Shell-Isolated Nanoparticles (SHINEF). *Angew. Chem. Int. Ed.* **50**, 665–668 (2011).
11. Furtaw, M. D., Steffens, D. L., Urlacher, T. M. & Anderson, J. P. A near-infrared, surface-enhanced, fluorophore-linked immunosorbent assay. *Anal. Chem.* **85**, 7102–7108 (2013).
12. Walsh, G. F. & Dal Negro, L. Enhanced Second Harmonic Generation by Photonic–Plasmonic Fano-Type Coupling in Nanoplasmonic Arrays. *Nano lett.* **13**, 3111–3117 (2013).
13. Shen, Y. Surface properties probed by second-harmonic and sum-frequency generation. *Nature* **337**, 519–525 (1989).
14. Geiger, F. M. Second harmonic generation, sum frequency generation, and χ (3): Dissecting environmental interfaces with a nonlinear optical Swiss Army knife. *Annu. Rev. Phys. Chem.* **60**, 61–83 (2009).
15. Kozuch, J., Steinem, C., Hildebrandt, P. & Millo, D. Combined Electrochemistry and Surface-Enhanced Infrared Absorption Spectroscopy of Gramicidin A Incorporated into Tethered Bilayer Lipid Membranes. *Angew. Chem. Int. Ed.* **51**, 8114–8117 (2012).
16. Brown, L. V. *et al*. Surface-enhanced infrared absorption using individual cross antennas tailored to chemical moieties. *J. AM. CHEM. SOC.* **135**, 3688–3695 (2013).
17. Richter, M. M. Electrochemiluminescence (ecl). *Chem. Rev.* **104**, 3003–3036 (2004).
18. Guo, L., Fu, F. & Chen, G. Capillary electrophoresis with electrochemiluminescence detection: fundamental theory, apparatus, and applications. *Anal. Bioanal. Chem.* **399**, 3323–3343 (2011).
19. Miao, W. Electrogenerated chemiluminescence and its biorelated applications. *Chem. Rev.* **108**, 2506–2553 (2008).
20. Crespo, G. N. A., Mistlberger, G. N. & Bakker, E. Electrogenerated chemiluminescence for potentiometric sensors. *J. AM. CHEM. SOC.* **134**, 205–207 (2011).
21. Chen, Z., Liu, Y., Wang, Y., Zhao, X. & Li, J. Dynamic Evaluation of Cell Surface N-Glycan Expression via an Electrogenerated Chemiluminescence Biosensor Based on Concanavalin A-Integrating Gold-Nanoparticle-Modified Ru (bpy) 32+-Doped Silica Nanoprobe. *Anal. Chem.* **85**, 4431–4438 (2013).
22. Wei, H. *et al*. [Ru (bpy) 3] 2+-Doped Silica Nanoparticles within Layer-by-Layer Biomolecular Coatings and Their Application as a Biocompatible Electrochemiluminescent Tag Material. *CHEM-EUR. J.* **14**, 3687–3693 (2008).
23. Guo, L. *et al*. Capillary electrophoresis with electrochemiluminescent detection for highly sensitive assay of genetically modified organisms. *Anal. Chem.* **81**, 9578–9584 (2009).
24. Wang, X. *et al*. A controllable solid-state Ru (bpy) 32+ electrochemiluminescence film based on conformation change of ferrocene-labeled DNA molecular beacon. *Langmuir* **24**, 2200–2205 (2008).
25. Hu, L. *et al*. [Ru (bpy) 2dppz] 2+ electrochemiluminescence switch and its applications for DNA interaction study and label-free ATP aptasensor. *Anal. Chem.* **81**, 9807–9811 (2009).
26. Guo, L., Qiu, B., Xue, L. & Chen, G. CE with a new electrochemiluminescent detection system for separation and detection of proteins labeled with tris (1, 10-phenanthroline) ruthenium (II). *Electrophoresis* **30**, 2390–2396 (2009).
27. Du, Y. *et al*. Microchip capillary electrophoresis with solid-state electrochemiluminescence detector. *Anal. Chem.* **77**, 7993–7997 (2005).
28. Lin, Z., Ino, K., Shiku, H., Matsue, T. & Chen, G. Addressable electrochemiluminescence detection system based on redox-cycling of Ru (bpy) 32+. *Chem. Commun.* **46**, 243–245 (2009).
29. Qi, W. *et al*. Electrochemiluminescence Resonance Energy Transfer Based on Ru (phen) 32+-Doped Silica Nanoparticles and Its Application in "Turn-on" Detection of Ozone. *Anal. Chem.* **85**, 3207–3212 (2013).
30. Zhao, L., Krishnan, S., Zhang, Y., Schenkman, J. B. & Rusling, J. F. Differences in metabolite-mediated toxicity of tamoxifen in rodents versus humans elucidated with DNA/microsome electro-optical arrays and nanoreactors. *Chem. Res. Toxicol.* **22**, 341–347 (2009).
31. Sardesai, N. P., Barron, J. C. & Rusling, J. F. Carbon nanotube microwell array for sensitive electrochemiluminescent detection of cancer biomarker proteins. *Anal. Chem.* **83**, 6698–6703 (2011).
32. Jiali Niu, T. Z., Zhongfan Liu. One-step seed-mediated growth of 30–150 nm quasispherical gold nanoparticles with 2-mercaptosuccinic acid as a new reducing agent. *Nanotechnology* **18**, 325607 (2007).
33. Workman, S. & Richter, M. M. The effects of nonionic surfactants on the tris (2, 2'-bipyridyl) ruthenium (II)-tripropylamine electrochemiluminescence system. *Anal. Chem.* **72**, 5556–5561 (2000).
34. Xu, G., Pang, H.-L., Xu, B., Dong, S. & Wong, K.-Y. Enhancing the electrochemiluminescence of tris (2, 2′-bipyridyl) ruthenium (II) by ionic surfactants. *Analyst* **130**, 541–544 (2005).
35. Sun, S. *et al*. Study of highly efficient bimetallic ruthenium tris-bipyridyl ecl labels for coreactant system. *Anal. Chem.* **81**, 10227–10231 (2009).
36. Zanarini, S. *et al*. Ru (bpy) 3 covalently doped silica nanoparticles as multicenter tunable structures for electrochemiluminescence amplification. *J. AM. CHEM. SOC.* **131**, 2260–2267 (2009).
37. Zhuo, Y. *et al*. Ultrasensitive Apurinic/Apyrimidinic Endonuclease 1 Immunosensing Based on Self-Enhanced Electrochemiluminescence of a Ru(II) Complex. *Anal. Chem.* **86**, 1053–1060 (2014).
38. Gui, G.-F. *et al*. In Situ Generation of Self-Enhanced Luminophore by β-Lactamase Catalysis for Highly Sensitive Electrochemiluminescent Aptasensor. *Anal. Chem.* **86**, 5873–5880 (2014).
39. Zhang, J., Gryczynski, Z. & Lakowicz, J. R. First observation of surface plasmon-coupled electrochemiluminescence. *Chem. phys. lett.* **393**, 483–487 (2004).
40. Chowdhury, M. H. *et al*. First observation of surface plasmon-coupled chemiluminescence (SPCC). *Chem. phys. lett.* **435**, 114–118 (2007).
41. Wang, J. *et al*. Gold nanoparticle enhanced electrochemiluminescence of CdS thin films for ultrasensitive thrombin detection. *Anal. Chem.* **83**, 4004–4011 (2011).
42. Shan, Y., Xu, J.-J. & Chen, H.-Y. Distance-dependent quenching and enhancing of electrochemiluminescence from a CdS: Mn nanocrystal film by Au nanoparticles for highly sensitive detection of DNA. *Chem. Commun.* **8**, 905–907 (2009).
43. Guo, L., Chen, G. & Kim, D.-H. Three-dimensionally assembled gold nanostructures for plasmonic biosensors. *Anal. Chem.* **82**, 5147–5153 (2010).
44. Guo, L. *et al*. Oriented gold nanoparticle aggregation for colorimetric sensors with surprisingly high analytical figures of merit. *J. AM. CHEM. SOC.* **135**, 12338–12345 (2013).
45. Jebb, M. *et al*. Ruthenium (II) trisbipyridine functionalized gold nanorods. Morphological changes and excited-state interactions. *J. Phys. Chem. B* **111**, 6839–6844 (2007).
46. Huang, T. & Murray, R. W. Quenching of [Ru (bpy) 3] 2+ fluorescence by binding to Au nanoparticles. *Langmuir* **18**, 7077–7081 (2002).

47. Anker, J. N. *et al.* Biosensing with plasmonic nanosensors. *Nat. Mater.* **7**, 442–453 (2008).
48. Ozbay, E. Plasmonics: merging photonics and electronics at nanoscale dimensions. *Science* **311**, 189–193 (2006).
49. Wang, J. *et al.* Gold nanoparticle enhanced electrochemiluminescence of CdS thin films for ultrasensitive thrombin detection. *Anal. Chem.* **83**, 4004–4011 (2011).
50. Miao, W., Choi, J.-P. & Bard, A. J. Electrogenerated Chemiluminescence 69: The Tris (2, 2'-bipyridine) ruthenium (II),(Ru (bpy) 32+)/Tri-n-propylamine (TPrA) System Revisited A New Route Involving TPrA+ Cation Radicals. *J. AM. CHEM. SOC.* **124**, 14478–14485 (2002).
51. Fort, E. & Grésillon, S. Surface enhanced fluorescence. *J. Phys. D: Appl. Phys.* **41**, 013001 (2008).
52. Gurunatha, K. L. & Dujardin, E. Tuning the Optical Coupling between Molecular Dyes and Metal Nanoparticles by the Templated Silica Mineralization of J-Aggregates. *J. Phys. Chem. C* **117**, 3489–3496 (2013).
53. Pelaz, B. *et al.* The State of Nanoparticle-Based Nanoscience and Biotechnology: Progress, Promises, and Challenges. *ACS nano* **6**, 8468–8483 (2012).
54. Lakowicz, J. R. Radiative decay engineering 5: metal-enhanced fluorescence and plasmon emission. *Anal. Biochem.* **337**, 171–194 (2005).
55. Xu, Y. *et al.* Facile preparation of partially functionalized gold nanoparticles via a surfactant-assisted solid phase approach. *J. Colloid Interf. Sci.* **409**, 32–37 (2013).
56. Gorelikov, I. & Matsuura, N. Single-step coating of mesoporous silica on cetyltrimethyl ammonium bromide-capped nanoparticles. *Nano Lett.* **8**, 369–373 (2008).

Acknowledgments

The authors gratefully acknowledge the financial support of the National Science Foundation of China (21277025, 21205017, 21375021, 21222506), National Key Technologies R & D Program of China during the 12th Five-Year Plan Period (2012BAD29B06, 2012BAK01B01), the Foundation of Fujian Educational Committee (JA12039, JA13024), and the Scientific Research Foundation for the Returned Overseas Chinese Scholars, State Education Ministry.

Author contributions

D.-F.W. and L.-H.G. designed the research; D.-F.W. and R.H. performed the experiments; D.-F.W. and L.-H.G. analyzed the data; R.H., B.Q., Z.-Y. L., and G.-N.C. contributed to the reagents/materials/ analysis tools; D.-F.W.and L.-H.G. wrote the paper; all authors approved the final manuscript.

Additional information

The electrochemical responses of different modified electrodes, SEECL observed in 30-nm sillica coating, and SEECL observed in other $Ru(bpy)_3^{2+}$-coreactant systems.

Supplementary information accompanies this paper at http://www.nature.com/scientificreports

Competing financial interests: The authors declare no competing financial interests.

How to cite this article: Wang, D. *et al.* Surface Enhanced Electrochemiluminescence of $Ru(bpy)_3^{2+}$. *Sci. Rep.* **5**, 7954; DOI:10.1038/srep07954 (2015).